GEOPHYSICS, VOL. 85, NO. 6 (NOVEMBER-DECEMBER 2020); P. J111–J120, 8 FIGS., 2 TABLES.
10.1190/GEO2020-0157.1

The positioning of buried pipelines from magnetic data

Caifang Li[1], Dejun Liu[1], Jin Meng[1], Jialin Liu[1], and Yan Zhang[1]

ABSTRACT

Buried pipelines are "lifelines" for cities; therefore, it is vital to understand their location and depth before municipal construction to prevent them from being damaged. Magnetic methods have been applied to detect buried ferrous metal pipelines such as steel and cast-iron pipes. We have developed a positioning method for buried pipelines from magnetic data, which is based on a combination of the tilt angle and the downward continuation. The magnetic tilt angle can provide information about the location and depth of buried pipelines, which can easily be calculated by the horizontal and vertical magnetic field gradients. We prove that the tilt angle for the magnetic field that has been reduced to the pole is independent of the magnetization direction given by the pipeline direction with respect to the inducing field. A tilt angle of 90° marks the location of a buried pipeline, whereas the depth is the distance between the location of the 90° and its adjacent 0°. The iterative Tikhonov regularization method for downward continuation, while separating the superimposed anomalies and enhancing the horizontal resolution, also reduces the influence of fast Fourier transform-induced noise and other noise that is intrinsic to the data set. We use the derivative of the Tikhonov regularization result as a regularization term of the minimization function and a constraint for the regularization parameter choice to obtain a more stable and accurate downward-continued result. This positioning method is applicable to single and parallel pipeline detection.

INTRODUCTION

Buried pipelines are "lifelines" for cities and are responsible for the transmission function of material and energy. It is vital to find their location and buried depth to prevent them from being damaged in the process of urban development and construction. Magnetic methods have been used for the positioning of buried ferrous metal pipelines.

Many methods have been developed to process sampled magnetic data to estimate source parameters. Nabighian (1972) calculates the depth, magnetic susceptibility, and dip of 2D bodies by using the analytic signal of the magnetic anomaly. Thompson (1982) proposes the Euler deconvolution method, which is based on the Euler's homogeneity relationship, to infer the depth of 2D sources from the magnetic data. This method requires assumption of a "structural index" related to the type of magnetic target. Salem and Ravat (2003) present a method based on a combination of the analytic signal method and the Euler deconvolution method to deduce the location, depth, and geometry of magnetic sources. Salem et al. (2004) use the linear equation between a symmetric anomalous field and its horizontal gradient to calculate the source's depth. The method is suitable for a single contact, a dike, and a horizontal cylinder. Miller and Singh (1994) introduce the concept of magnetic tilt angle, which estimates the location and depth of vertical contacts based on the ratio of the vertical and horizontal gradients of the magnetic field. Salem et al. (2007) and Cooper (2014) apply the tilt angle to identify the source of an infinite contact. Salem et al. (2008) combine the tilt angle with the Euler deconvolution method to identify the location, depth, and shape of magnetic sources without a priori information about the structural index of the target. Salem et al. (2013) and Murphy et al. (2012) describe an adaptive tilt angle equation for depth estimating from full-tensor gravity data. This method is suitable for estimating the location and depth of a single point mass, a horizontal line of mass, a vertical sheet, and a horizontal sheet. Cooper (2016) describes the downward continuation of the tilt angle, which allows more accurate sources depth determination from the tilt-depth method, but it is strictly valid only for isolated sources. Eshaghzadeh (2017) applies the tilt derivative to estimate the depth of a semi-infinite vertical cylindrical.

With the rapid development of cities, the underground space available for urban construction is becoming more and more limited. Most pipelines are buried in parallel to economize urban underground

Manuscript received by the Editor 11 March 2020; revised manuscript received 11 August 2020; published ahead of production 9 September 2020; published online 10 November 2020.
[1]China University of Petroleum-Beijing, State Key Laboratory of Petroleum Resources and Prospecting, Changping 102249, Beijing, China and China University of Petroleum-Beijing, College of Information Science and Engineering, Changping 102249, Beijing, China. E-mail: licf93@163.com; liudj65@163.com (corresponding author); 1010548233@qq.com; 2500417740@qq.com; 1114162607@qq.com.

space resources. The major difficulty for identifying parallel pipelines is that the magnetic anomalies generated by them are superimposed on each other. Downward continuation can separate superimposed magnetic anomalies and enhance horizontal resolution. Dean (1958) derives the frequency response of the downward continuation of the potential field and points out that the approach represents an ill-posed problem. Many methods exist for stabilizing the downward-continuation process. Tikhonov et al. (1968) introduce a stable downward-continuation method based on the classic regularization concept. Cooper (2004) suggests three methods for stable downward continuation, and the results show that downward continuation achieved by least-squares inversion is more stable. Pasteka et al. (2012) use C-norms to select the optimum regularization parameter value of the Tikhonov regularization method. Xu et al. (2007) introduce an iterative method for downward continuation that is more stable than the Fourier transform method and able to downward continue data to a greater depth. Zeng et al. (2013) prove that the iterative downward-continuation method is sensitive to noise and develop an adaptive iterative method based on Tikhonov regularization approach, which allows the control of fast Fourier transform (FFT)-induced noise and other noise that is intrinsic to the data set. Cooper (2019) introduces a downward-continuation algorithm that downward continues the data by a distance that is a fraction of the current depth, rather than by a fixed distance.

The main goal of magnetic surveying of buried pipelines is to estimate their location and depth based on acquired data. In this paper, we describe a positioning method for buried pipelines from magnetic data, which is based on a combination of tilt angle and downward continuation. Compared with other interpretation methods, such as Euler deconvolution and optimization inversion, our method does not need to consider pipeline demagnetization and the pipeline direction with respect to the inducing field. In addition, while performing the iterative Tikhonov-regularization for data downward continuation, we replace the Tikhonov-regularization result with its derivative as a regularization term of the minimization function and a constraint for the regularization parameter choice to ensure that the downward-continued result is more stable and accurate.

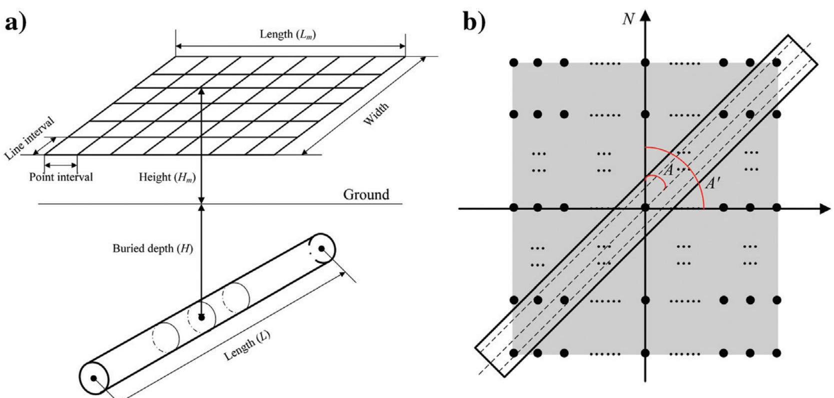

Figure 1. The magnetic measurement model of a single buried pipeline: (a) aide view and (b) top view.

Table 1. The values of a single buried pipeline's model parameters.

Model parameters		Value
Pipeline	Length (L)	50 m
	Outer diameter	0.3 m
	Thickness	0.02 m
	Density	7860 kg/m^3
	Magnetic susceptibility	1 SI
	Azimuth (A)	60°
	Buried depth (H)	3 m
Inducing field	Intensity	55,000 nT
	Inclination (I)	−30°
Measurement plane	Length (L_m)	10 m
	Width	10 m
	Height (H_m)	0 m
	Azimuth (A')	90°
	Measurement point interval	0.1 m
	Measurement line interval	0.1 m

BASIC THEORIES

Magnetic tilt angle

When the length of a pipeline is much longer than its buried depth, it can be regarded as an infinite horizontal cylinder. Assuming that the pipeline runs parallel to the y-axis, the gravitational potential V generated by the pipeline at any observation point $P(x, y, z)$ can be expressed as (Nagy et al., 2000)

$$V(x, y, z) = -2G\rho S \cdot \ln r, \tag{1}$$

where G is the gravitational constant, ρ is the density of the pipeline, $S = \pi\delta(\Phi - \delta)$ is the cross-section area of the pipeline, Φ and δ are the outer diameter and thickness of the pipeline, $r = \sqrt{(x - X)^2 + (z - H)^2} = \sqrt{\Delta x^2 + \Delta z^2}$, X and H are the location and buried depth of the pipeline.

There are two assumptions: (1) The pipeline has uniform magnetic susceptibility κ, and (2) the remanent magnetization M_r and the induced magnetization M_i have the same direction. Therefore, the magnetization M of the pipeline can be expressed as (Wang et al., 2019)

$$M = M_i + M_r = \kappa \frac{T_0}{\mu_0} + M_r, \tag{2}$$

where μ_0 is the permeability of the vacuum and T_0 is the inducing field.

The components of the magnetization M in the x-, y-, and z-directions are

$$M_x = M \cos I \sin A, \ \ M_y = M \cos I \cos A, \ \ M_z = M \sin I, \tag{3}$$

where I is the inclination of the inducing field and A is the azimuth of the pipeline (i.e., the angle between the pipeline direction and magnetic north A is positive eastward).

According to Poisson's equation, there is a relationship between the magnetic and gravitational potentials of the pipeline (Wang et al., 2019). The magnetic potential of the pipeline is

$$U = \frac{-1}{4\pi G\rho} M \cdot \mathrm{grad}_p V, \tag{4}$$

and the magnetic field of the pipeline is

$$B = -\mu_0 \nabla U. \tag{5}$$

Because the pipeline is running parallel to the y-axis, the gravitational potential along the pipeline direction (the y-axis) is

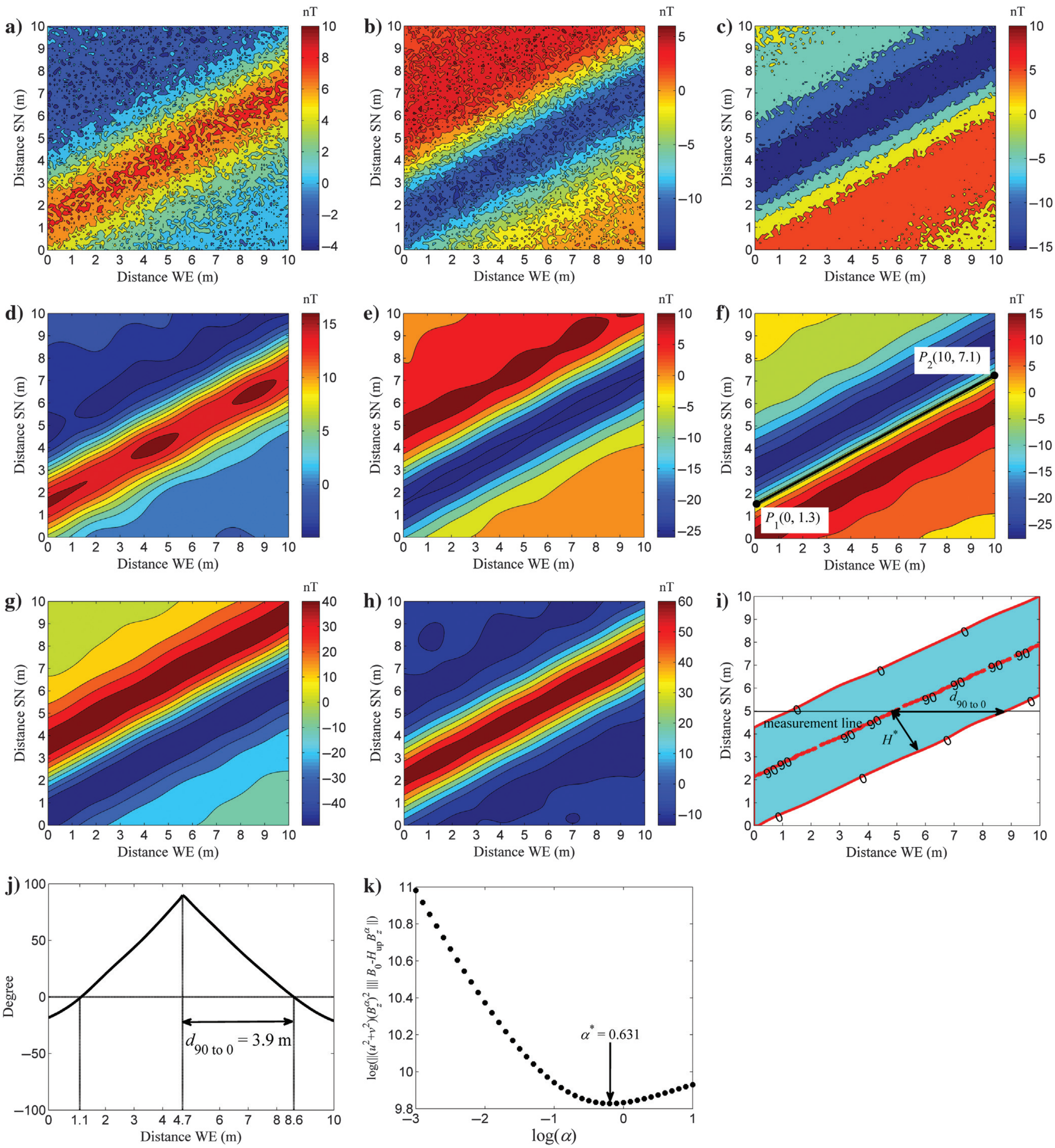

Figure 2. (a-c) The responses of B_{mx}, B_{my}, and B_{mz}, corrupted by random noise with 1nT standard deviation and 1nT average, (d-f) data from (a), (b), and (c) downward continued by 1 m, respectively, (g-h) pole-reduced data $B_{x\perp}$ and $B_{z\perp}$, (i) tilt angle map, (j) tilt angle curve on the measurement line drawn in Figure 2i, and (k) the curve of the regularization parameters.

unchanged and the y-directional second-order partial derivatives are zero. The components of the magnetic field B in the x-, y-, and z-directions are as follows:

$$B_z = \frac{\mu_0}{4\pi G\rho}(M_x V_{xz} + M_z V_{zz}),$$
$$B_x = \frac{\mu_0}{4\pi G\rho}(M_x V_{xx} + M_z V_{xz}), \quad B_y = 0, \tag{6}$$

where V_{xx}, V_{xz}, and V_{zz} are second-order derivatives of the gravity potential V, $V_{xx} = -V_{zz}$.

Substituting equations 1 and 3 into 6, we get

$$B_z = \frac{\mu_0 SM[2\cos I \sin A \cdot \Delta x \Delta z - \sin I(\Delta x^2 - \Delta z^2)]}{2\pi(\Delta x^2 + \Delta z^2)^2}, \tag{7}$$

$$B_x = \frac{\mu_0 SM[\cos I \sin A(\Delta x^2 - \Delta z^2) + 2\sin I \cdot \Delta x \Delta z]}{2\pi(\Delta x^2 + \Delta z^2)^2}. \tag{8}$$

When the pipeline is vertically magnetized, $M_x = 0$, $M_z = M$, and

$$B_{z\perp} = \frac{\mu_0}{4\pi G\rho} M V_{zz}, \quad B_{x\perp} = \frac{\mu_0}{4\pi G\rho} M V_{xz}. \tag{9}$$

Substituting equations 3 and 9 into 6, we get

$$B_z = B_{x\perp}\cos I \sin A + B_{z\perp}\sin I,$$
$$B_x = B_{x\perp}\sin I - B_{z\perp}\cos I \sin A, \tag{10}$$

and the equation for reducing magnetic data to the pole:

$$B_{z\perp} = \frac{B_z \sin I - B_x \cos I \sin A}{\sin^2 I + \cos^2 I \sin^2 A}, \quad B_{x\perp} = \frac{B_z \cos I \sin A + B_x \sin I}{\sin^2 I + \cos^2 I \sin^2 A}. \tag{11}$$

Figure 3. An exposed buried pipeline in the Changping District, Beijing.

Substituting equations 7 and 8 into 11, we get

$$B_{z\perp} = (\Delta z^2 - \Delta x^2)\frac{\mu_0 MS(1 - \cos^2 A \cos^2 I)}{2\pi(\Delta x^2 + \Delta z^2)^2(\sin^2 I + \cos^2 I \sin^2 A)}, \tag{12}$$

$$B_{x\perp} = 2\Delta x \Delta z \frac{\mu_0 MS(1 - \cos^2 A \cos^2 I)}{2\pi(\Delta x^2 + \Delta z^2)^2(\sin^2 I + \cos^2 I \sin^2 A)}. \tag{13}$$

The tilt angle can be expressed as (Miller and Singh, 1994)

$$\theta = \tan^{-1}\left(\frac{B_z}{\sqrt{B_x^2 + B_y^2}}\right). \tag{14}$$

Substituting equations 12 and 13 into 14, we get

$$\theta = \tan^{-1}\left(\frac{\Delta z^2 - \Delta x^2}{|2\Delta x \Delta z|}\right). \tag{15}$$

The tilt angle for pole-reduced magnetic data is the same as the tilt angle for full tensor gravity data (Murphy et al., 2012), which is not affected by the magnetization direction given by the pipeline direction with respect to the inducing field. A tilt angle of 90° ($\Delta x = 0$) marks the location of a buried pipeline, whereas its depth is the distance between the location of the 90° and its adjacent 0° ($\Delta x = \Delta z$).

In real magnetic measurements, measurement lines are usually not perpendicular to the buried pipeline. Therefore, the data should be rotated using equation 16 before reducing to the pole:

$$\begin{bmatrix} B_x \\ B_y \\ B_z \end{bmatrix} = \begin{bmatrix} \sin(A' - A) & \cos(A' - A) & 0 \\ \cos(A' - A) & -\sin(A' - A) & 0 \\ 0 & 0 & 1 \end{bmatrix} \begin{bmatrix} B_{mx} \\ B_{my} \\ B_{mz} \end{bmatrix}, \tag{16}$$

where A' is the azimuth of the measurement line (that is the angle between the measurement line direction and magnetic north, A' is positive eastward), and B_{mx}, B_{my}, and B_{mz} are the magnetic observation data. The azimuth A of the pipeline can be calculated as (Guo et al., 2015a)

$$A = \arctan\frac{x_{p2} - x_{p1}}{y_{p2} - y_{p1}}, \tag{17}$$

where $P_1(x_{p1}, y_{p1})$ and $P_2(x_{p2}, y_{p2})$ are the coordinates of two points of a contour line in the magnetic map.

Downward continuation

If the magnetic data on the measurement plane are denoted by $B(x, y, z_0)$, the magnetic data $B(x, y, z)$ on any plane can be obtained from equation 18 (Dean, 1958):

$$B(x, y, z) = \frac{\Delta h}{2\pi}\int_{-\infty}^{\infty}\int_{-\infty}^{\infty}\frac{B(\varepsilon, \eta, z_0)}{[(x-\varepsilon)^2 + (y-\eta)^2 + \Delta h^2]^{3/2}} d\varepsilon d\eta, \tag{18}$$

where $\Delta h = z_0 - z$ is the elevation difference and the z-axis is positive downward.

An integral kernel function $k(x, y)$ is defined as

$$k(x, y) = \frac{\Delta h}{2\pi} \cdot \frac{1}{(x^2 + y^2 + \Delta h^2)^{3/2}}. \tag{19}$$

Therefore, equation 18 can be written as a convolution:

$$B(x, y, z) = k(x, y) \otimes B(x, y, z_0). \tag{20}$$

In the frequency domain, equation 20 can be written as a product:

$$\hat{B}(u, v, z) = H(u, v)\hat{B}(u, v, z_0), \tag{21}$$

and

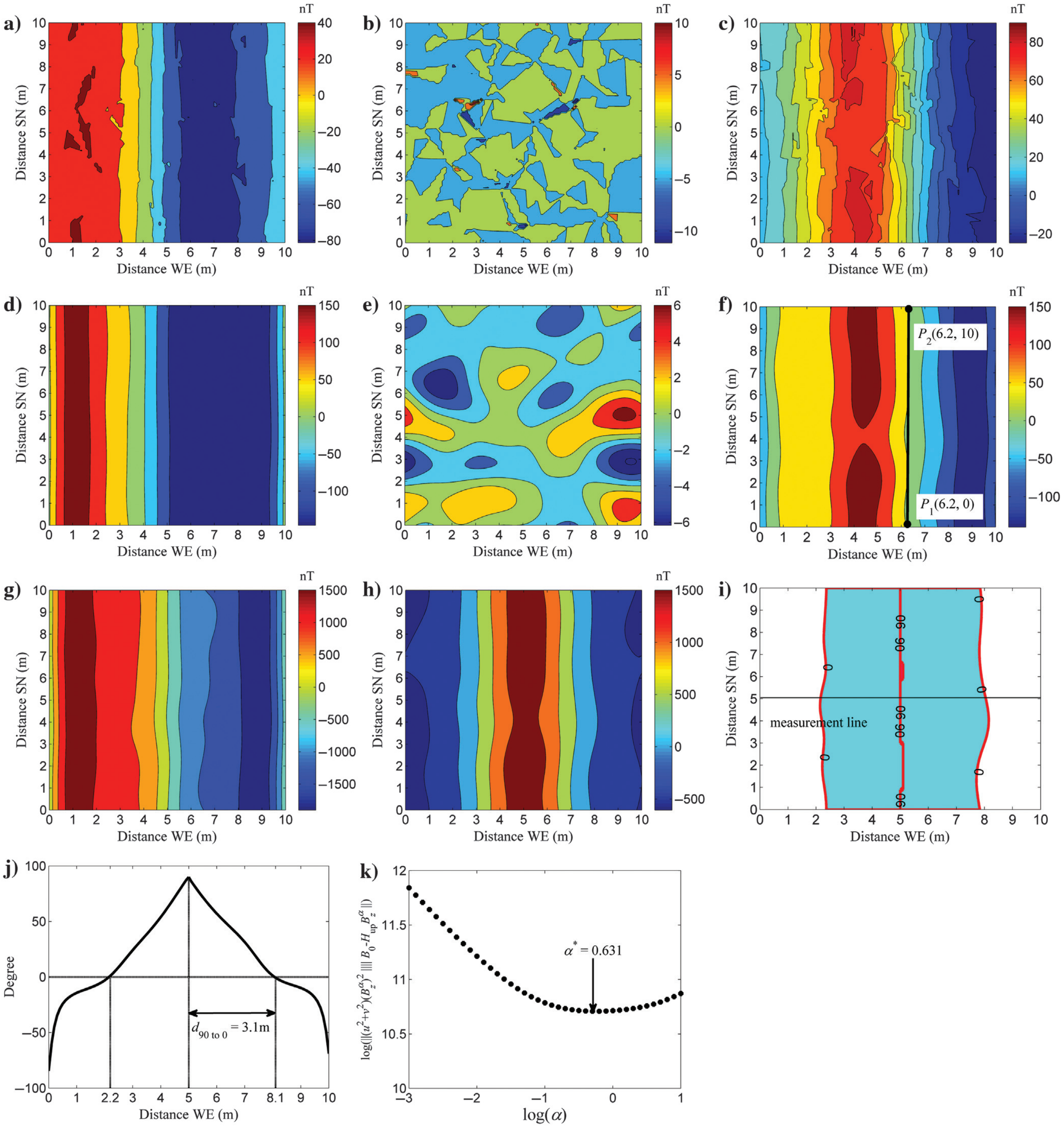

Figure 4. (a-c) The responses of B_{mx}, B_{my}, and B_{mz}, (d-f) data from (a-c) downward continued by 1.5 m, respectively, (g-h) pole-reduced data $B_{x\perp}$ and $B_{z\perp}$, (i) tilt angle map, (j) tilt angle curve on the measurement line drawn in panel i, and (k) the curve of the regularization parameters.

$$H(u,v) = e^{-2\pi\cdot\Delta h\cdot\sqrt{u^2+v^2}}, \tag{22}$$

where $\hat{B}(u,v,z)$, $\hat{B}(u,v,z_0)$, and $H(u,v)$ are the Fourier transforms of $B(x,y,z)$, $B(x,y,z_0)$, and $k(x,y)$ and u and v are the wavenumbers in the x- and y-axes.

When Δh is positive (or negative), equation 21 is the calculation for upward (or downward) continuation and equation 22 is the upward-continuation operator $H_{\mathrm{up}}(u,v)$ (or the downward-continuation operator $H_{\mathrm{down}}(u,v)$). The downward continuation, while enhancing details in the data, also amplifies high-frequency noise. Consequently, one needs to regularize the problem to obtain a reasonable approximate solution. The most popular method is Tikhonov regularization, which for downward continuation allows the control of FFT-induced noise and other noise intrinsic to the data set.

The Tikhonov-regularization approach can be defined as a minimization problem solution — we must minimize a function (J), which is formulated as (Tikhonov and Arsenin, 1977)

$$\iint_D J\left[x,y,B_z,\frac{\partial B_z}{\partial x},\frac{\partial B_z}{\partial y}\right]dxdy = \iint_D \left\{[k(x,y)\otimes B_z - B_0]^2 + \alpha\left[\left(\frac{\partial B_z}{\partial x}\right)^2 + \left(\frac{\partial B_z}{\partial y}\right)^2\right]\right\}dxdy = \min, \tag{23}$$

where $B_z = B(x,y,z)$, $B_0 = B(x,y,z_0)$; $\alpha > 0$ is the regularization parameter, which provides a trade-off between the measurement fidelity and the prior information introduced by the regularizing function.

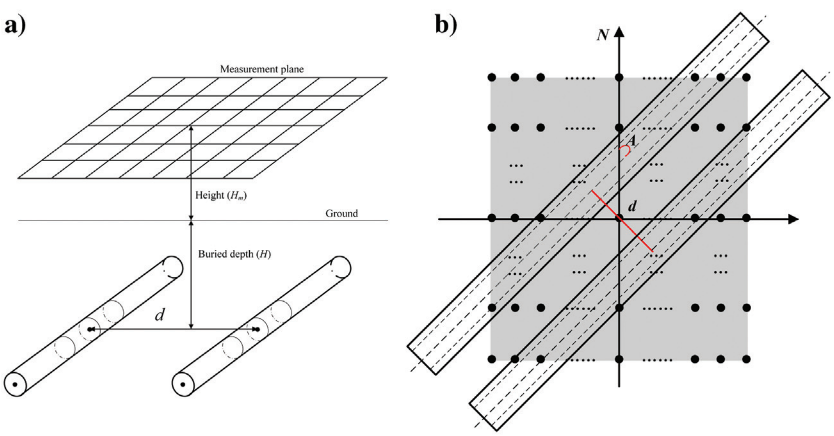

Figure 5. The magnetic measurement model of parallel buried pipelines: (a) side view and (b) top view.

Table 2. The values of the parallel buried pipelines' model parameters.

Model parameters			
Induced field inclination (I)	Azimuth (A)	Buried depth (H)	Axis spacing (d)
45°	−45°	2 m	1 m

The Euler-Lagrange equation corresponding to equation 23 is (Troutman, 1983)

$$\begin{aligned}&\frac{\partial J}{\partial B_z} - \frac{\partial}{\partial x}\left(\frac{\partial J}{\partial(\partial B_z/\partial x)}\right) - \frac{\partial}{\partial y}\left(\frac{\partial J}{\partial(\partial B_z/\partial y)}\right)\\ &= \left\{2[k(x,y)\otimes B_z - B_0]\cdot\frac{\partial[k(x,y)\otimes B_z]}{\partial B_z}\right\} - 2\alpha\frac{\partial^2 B_z}{\partial x^2} - 2\alpha\frac{\partial^2 B_z}{\partial y^2}\\ &= k(x,y)\otimes B_z - B_0 - \alpha\left(\frac{\partial^2 B_z}{\partial x^2} + \frac{\partial^2 B_z}{\partial y^2}\right)\\ &= 0,\end{aligned} \tag{24}$$

where

$$\frac{\partial(k(x,y)\otimes B_z)}{\partial B_z} = \frac{1}{2\pi}\int_{-\infty}^{\infty}\int_{-\infty}^{\infty}\frac{\Delta h}{[(x-\xi)^2+(y-\eta)^2+\Delta h^2]^{3/2}}d\xi d\eta = 1.$$

Applying the Fourier transform to equation 24 and combining the theorem of spectrum of differentiation,

$$\frac{\partial^2 B_z}{\partial x^2} = (iu)^2\hat{B}_z = -u^2\hat{B}_z, \quad \frac{\partial^2 B_z}{\partial y^2} = (iv)^2\hat{B}_z = -v^2\hat{B}_z, \tag{25}$$

we get

$$H_{\mathrm{up}}\hat{B}_z + \alpha(u^2+v^2)\hat{B}_z = \hat{B}_0, \tag{26}$$

$$\hat{B}_z = \frac{\hat{B}_0}{H_{\mathrm{up}} + \alpha(u^2+v^2)} = H_{\mathrm{Tdown}}\hat{B}_0, \tag{27}$$

and

$$H_{\mathrm{Tdown}} = \frac{e^{-2\pi\cdot\Delta h\cdot\sqrt{u^2+v^2}}}{1+\alpha(u^2+v^2)e^{-2\pi\cdot\Delta h\cdot\sqrt{u^2+v^2}}}, \tag{28}$$

where $\hat{B}_z = \hat{B}(u,v,z)$ and $\hat{B}_0 = \hat{B}(u,v,z_0)$; $H_{\mathrm{Tdown}}(u,v)$ is the Tikhonov downward-continuation operator; and Δh is a negative number.

A saturation result of the Tikhonov regularization method shows that a higher rate of convergence cannot be expected under higher smoothness assumptions. However, a higher rate of convergence can be obtained by "iterative Tikhonov regularization" (Zeng et al., 2013), which is defined as follows:

$$\hat{B}_z^0 = H_{\mathrm{Tdown}}\hat{B}_0, \quad \hat{B}_z^n = \hat{B}_z^{n-1} + H_{\mathrm{Tdown}}(\hat{B}_0 - H_{\mathrm{up}}\hat{B}_z^{n-1}). \tag{29}$$

For the regularization method, the choices of the iteration number and the regularization parameter are crucial to yield a well-posed solution. The optimal iteration number is five. The root meansquare error between the downward-continued and theoretical fields is unchanged as the iteration number increases from five (Zeng et al., 2013). Here, we extended the algorithm for determining a regularization parameter as (Reginska, 1996)

$$\alpha^{*} = \arg\min\{\|(u^2+v^2)(\hat{B}_z^{\alpha})^2\|\|\hat{B}_0 - H_{\mathrm{up}}\hat{B}_z^{\alpha}\|\}. \tag{30}$$

APPLICATION TO A SINGLE BURIED PIPELINE

The depth-detection error is defined as the absolute difference between the estimated and true values for the buried depth of pipelines, which shall not exceed 0.15 H (in which H is the actual depth of buried pipelines. When $H < 1$ m, assume that $H = 1$ m) (Li et al., 2019). The location detection error is defined as the absolute

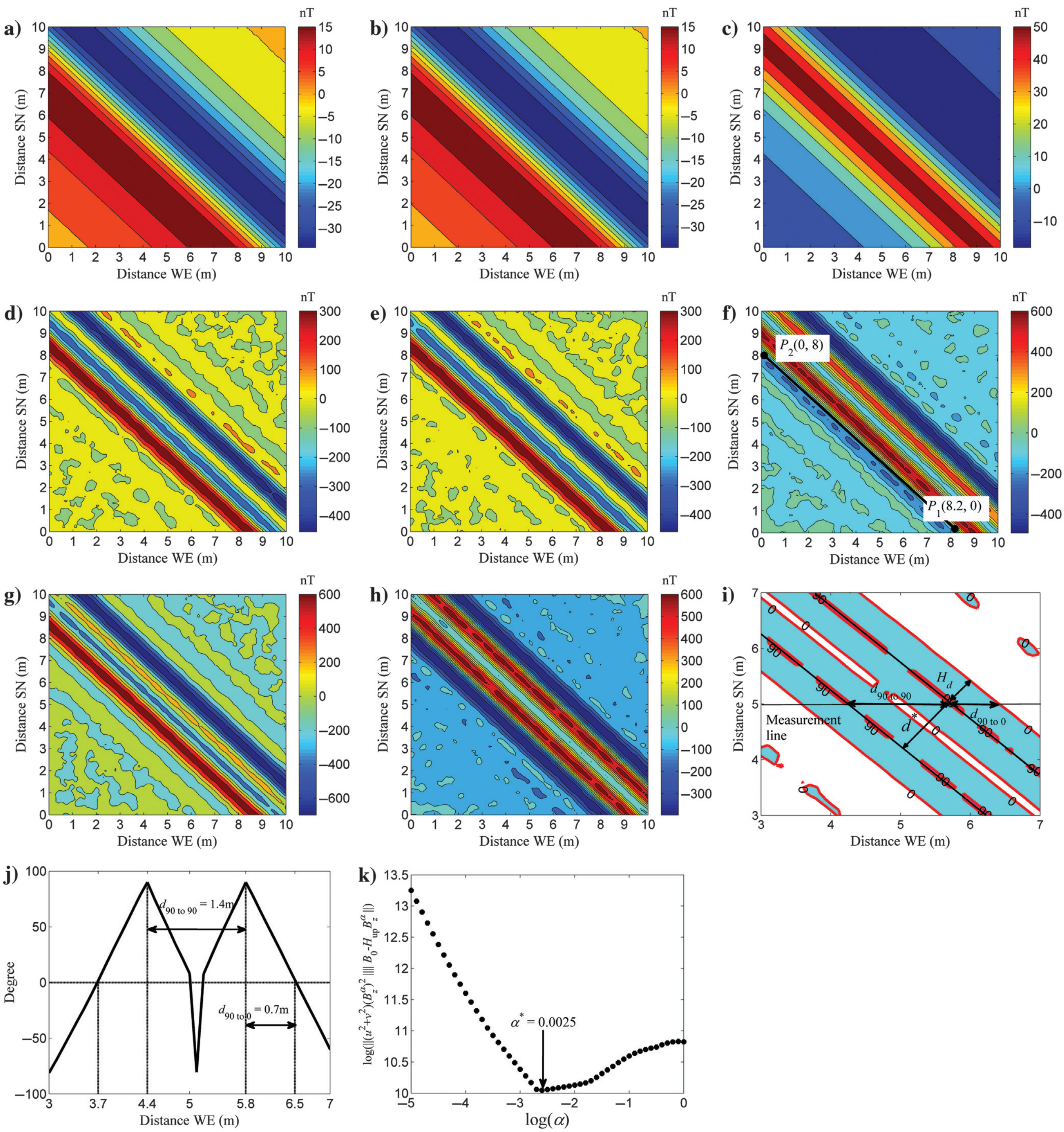

Figure 6. (a-c) The responses of B_{mx}, B_{my}, and B_{mz}, corrupted by noise with 0.01 nT standard, (d-f) data from (a-c) downward continued by 1.7 m, respectively, (g-h) pole-reduced data $B_{x\perp}$ and $B_{z\perp}$, (i) tilt angle map, (j) tilt angle curve on the measurement line drawn in panel i, and (k) the curve of the regularization parameters.

difference between the estimated and true values for the axis spacing of parallel pipelines, which shall not exceed 0.1 H.

We lower the downward-continuation altitude from zero at the measurement point interval. Because the data are downward continued closer to the pipeline depth, they contain more high-frequency detail that might be controlled in the process of the Tikhonov-regularization approach. Therefore, if the tilt angle map has one or two linear peaks with a value of 90°, we will stop lowering the downward-continuation altitude to avoid the increase of detection errors due to data distortion.

Theoretical example

The magnetic measurement model of a single buried pipeline is shown in Figure 1, in which the N-axis is the magnetic north, the gray area is a measurement plane, and the black spots are measurement points. The values of the model parameters are shown in Table 1.

Figure 2a-2c shows the response of the three components of the magnetic anomaly from the model presented in Figure 1, all of them corrupted by random noise with a standard deviation of 1nT and an average of 1nT. Figure 2d-2f are data from Figure 2a-2c downward continued by 1 m ($\Delta h = -1$ m) using equation 30 with $\alpha^* = 0.631$ (see Figure 2k), respectively. The terms $P_1(0, 1.3)$ and $P_2(10, 7.1)$ are the coordinates of two points of the contour line drawn in Figure 2f. The azimuth of the pipelines is determined to be 59.89° by equation 17. Figure 2g and 2h are the pole-reduced data calculated using equations 16 and 11 based on the data from Figure 2d-2f. Figure 2i is the tilt angle map of the data from Figure 2g and 2h computed using equation 14.

An estimated value of the buried depth of the pipeline can be determined as (see Figure 2i)

$$H^* = H_d + |\Delta h| - H_m = |d_{90\text{ to }0} \times \sin(A' - A)| + |\Delta h| - H_m, \quad (31)$$

where H_d is the depth from the downward-continuation plane to the pipeline, H_m is the height of the measurement plane, $d_{90\text{ to }0}$ is the distance between the location of the tilt angle value of 90° and its adjacent zero value, A' and A are the azimuth of the measurement line and the pipeline, respectively, and Δh is the downward-continuation distance.

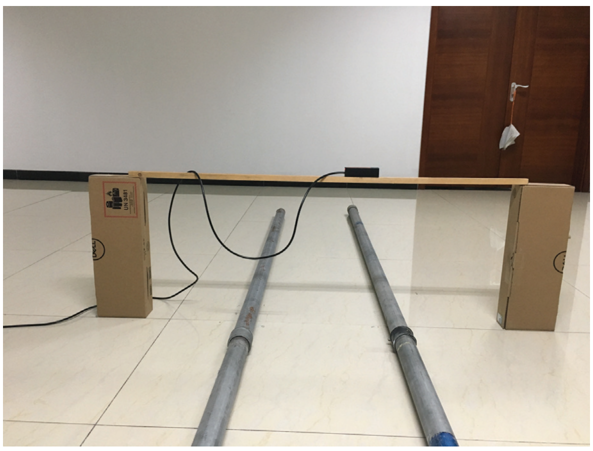

Figure 7. Two parallel cast-iron pipes on a flat area in our office building in the Changping District, Beijing.

The estimated value of the buried depth of the pipeline presented in Figure 1 is determined to be 2.95 m by equation 31. The depth detection error is 0.05 m, which is less than the precision of 0.45 m (i.e., 0.15 H, $H = 3$ m).

Field example

Figure 3 shows an exposed buried pipeline in the Changping District, Beijing. The pipeline running from north to south is buried at a depth of 4.5 m. The inclination and declination of the geomagnetic field are 59.061° and –6.629° (Guo et al., 2015b). The magnetic data acquisition equipment includes a computer and a measurement apparatus that is assembled by eight magnetoresistive sensors at an interval of 0.1 m in a straight line. We kept the measurement apparatus close to the ground and moved it along the east–west direction in the measurement area.

Figure 4a–4c shows the response of the horizontal and vertical components of the measured magnetic field. Figure 4d–4f are data from Figure 4a–4c downward continued by 1.5 m ($\Delta h = -1.5$ m) using equation 30 with $\alpha^* = 0.631$ (see Figure 4k), respectively. The coordinates of two points of the contour line drawn in Figure 4f are $P_1(6.2, 0)$ and $P_2(6.2, 10)$. The azimuth of the pipelines is determined to be 0° by equation 17. Figure 4g and 4h are the pole-reduced data calculated using equations 16 and 11 based on the data from Figure 4d-4f. Figure 4i is the tilt angle map of the data from Figure 4g and 4h computed using equation 14. The estimated value of the buried depth of the pipeline presented in Figure 3 is determined to be 4.6 m by equation 31. The depth detection error is 0.1 m, which is less than the precision of 0.675 m (i.e., 0.15 H, $H = 4.5$ m).

APPLICATION TO PARALLEL BURIED PIPELINES

Theoretical example

The magnetic measurement model of parallel buried pipelines is shown in Figure 5. The values of the fixed model parameters are shown in Table 1, and the values of the varying model parameters are shown in Table 2.

Figure 6a-6c shows the response of the three components of the magnetic anomaly from the model presented in Figure 5, all of them corrupted by random noise with a standard deviation of 0.01nT. Figure 6d-6f are data from Figure 6a-6c downward continued by 1.7 m ($\Delta h = -1.7$ m) using equation 30 with $\alpha^* = 0.0025$ (see Figure 6k), respectively. The terms $P_1(8.2, 0)$ and $P_2(0, 8)$ are the coordinates of two points of the contour line drawn in Figure 6f. The azimuth of the pipelines is determined to be −45.71° by equation 17. Figure 6g and 6h are the pole-reduced data calculated using equations 16 and 11 based on the data from Figure 6d-6f. Figure 6i is the tilt angle map of the data from Figure 6g and 6h computed using equation 14.

The estimated value of the axis spacing of the two pipelines can be determined as (see Figure 6i)

$$d^* = |d_{90\text{ to }90} \times \sin(A' - A)|, \quad (32)$$

where $d_{90\text{ to }90}$ is the distance between the locations of the tilt angle value of 90°.

The estimated values of the buried depth and axis spacing of the two pipelines presented in Figure 5 are determined to be 2.19 and 0.98 m by equations 31 and 32, respectively. The depth detection error is 0.19 m, which is less than the precision of 0.35 m (i.e., 0.15 H, $H = 2$ m). The location detection error is 0.02, which is less than the precision of 0.2 m (i.e., 0.1 H).

Experimental example

The magnetic-data-acquisition equipment used in the experiment includes an integrated magnetic gradiometer and a fluxgate sensor. The experiment was carried out on a flat area in our office building in the Changping District, Beijing (see Figure 7). The two pipes run from east to west. The buried depth and axis spacing of the two pipes are 0 and 0.5 m, respectively. The height of the measurement plane is 0.5 m. Measurement lines run from south to north. The three components B_x, B_y, and B_z observed by the equipment away from the pipes are 29556nT, –3424nT, and 52146nT, respectively.

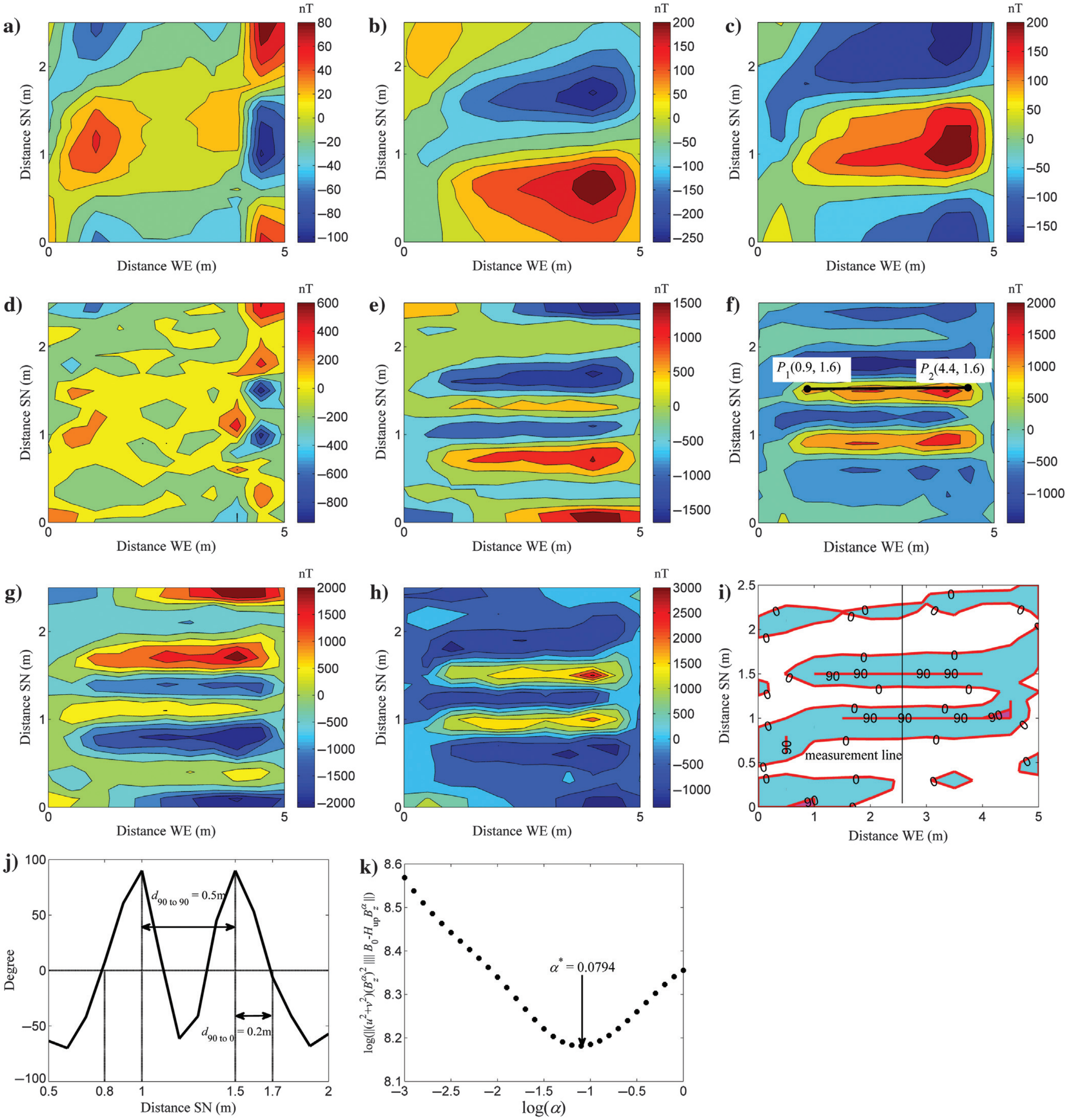

Figure 8. (a-c) The responses of B_{mx}, B_{my}, and B_{mz}, (d-f) data from (a-c) downward continued by 0.4 m, respectively, (g-h) pole-reduced data $B_{x\perp}$ and $B_{z\perp}$, (i) tilt angle map, (j) tilt angle curve on the measurement line drawn in panel i, and (k) the curve of the regularization parameters.

Substituting the three values into equation 33, we determine the inclination and declination of the geomagnetic field to be approximately 60° and −7°:

$$I = \arctan\frac{B_z}{\sqrt{B_x^2 + B_y^2}}, \qquad D = \arctan\frac{B_y}{B_x}. \tag{33}$$

Figure 8a–8c shows the response of the horizontal and vertical components of the measured magnetic field. Figure 8d–8f are data from Figure 8a-8c downward continued by 0.4 m ($\Delta h = -0.4$ m) using equation 30 with $\alpha^* = 0.0794$ (see Figure 8k), respectively. The coordinates of two points of the contour line drawn in Figure 8f are $P_1(0.9, 1.6)$ and $P_2(4.4, 1.6)$. The azimuth of the pipelines is determined to be 90° by equation 17. Figure 8g and 8h are the pole-reduced data calculated using equations 16 and 11 based on the data from Figure 8d–8f. Figure 8i is the tilt angle map of the data from Figure 8g and 8h computed using equation 14.The estimated value of the buried depth and axis spacing of the two pipes presented in Figure 7 are determined to be 0.1 and 0.5 m by equation 31 and 32, respectively. The depth detection error is 0.1 m, which is less than the precision of 0.15 m (i.e., 0.15 H, replace H with 1 m). The location detection error is 0 m, which meets the precision.

CONCLUSION

A positioning method for buried ferrous metal pipelines has been described based on a combination of magnetic tilt angle and downward continuation. The tilt angle of pole-reduced magnetic data for buried depth and location detection is not affected by the magnetization direction of pipelines. The iterative Tikhonov-regularization method for downward continuation not only enhances detail in magnetic data but allows the control of high-frequency noise. The application of the method to the positioning of single and parallel pipelines gave satisfactory results.

ACKNOWLEDGMENTS

We thank all of the reviewers and editors for their useful suggestions that improved this paper. This work was supported by the National Natural Science Foundation of China (no. 41374151 and no. 41074099).

DATA AND MATERIALS AVAILABILITY

Data associated with this research are available and can be accessed via the following URL: https://github.com/Licf93/Positioning.

REFERENCES

Cooper, G., 2004, The stable downward continuation of potential field data: Exploration Geophysics, **35**, 260–265, doi: 10.1071/EG04260.

Cooper, G., 2016, The downward continuation of the tilt angle: Near Surface Geophysics, **14**, 385–390, doi: 10.3997/1873-0604.2016022.

Cooper, G. R. J., 2014, Determining the location, depth, and dip of contacts from aeromagnetic data: Geophysics, **79**, no. 3, J35–J41, doi: 10.1190/geo2013-0181.1.

Cooper, G. R. J., 2019, The downward continuation of aeromagnetic data from magnetic source ensembles: Near Surface Geophysics, **17**, 101–107, doi: 10.1002/nsg.12035.

Dean, W. C., 1958, Frequency analysis for gravity and interpretation magnet: Geophysics, **23**, 97–127, doi: 10.1190/1.1438457.

Eshaghzadeh, A., 2017, Depth estimation using the tilt angle of gravity field due to the semi-infinite vertical cylindrical source: Journal of Geological Research, **2017**, no. 3513272, 1–7, doi: 10.1155/2017/3513272.

Guo, Z. Y., D. J. Liu, Q. Pan, Y. Y. Zhang, Y. Li, and Z. Wang, 2015a, Vertical magnetic field and its analytic signal applicability in oil field underground pipeline detection, Journal of Geophysics and Engineering: **12**, 340–350, doi: 10.1088/1742-2132/12/3/340.

Guo, Z. Y., D. J. Liu, Q. Pan, and Y. Y. Zhang, 2015b, Forward modeling of total magnetic anomaly over a pseudo-2D underground ferromagnetic pipeline: Journal of Applied Geophysics, **113**, 14–30, doi: 10.1016/j.jappgeo.2014.12.011.

Li, C. F., D. J. Liu, Y. Zhai, Y. Xie, and Y. Sun, 2019, The effect of parallel pipeline parameters on the characteristics of gravity and magnetic surveys: Journal of Applied Geophysics, **166**, 77–88, doi: 10.1016/j.jappgeo.2019.04.023.

Miller, H. G., and V. Singh, 1994, Potential field tilt — A new concept for location of potential field sources: Journal of Applied Geophysics, **32**, 213–217, doi: 10.1016/0926-9851(94)90022-1.

Murphy, C., J. Dickinson, and A. Salem, 2012, Depth estimating full tensor gravity data with the adaptive tilt angle method: ASEG, Extended Abstracts, 1–3, doi: 10.1071/ASEG2012ab166.

Nabighian, M. N., 1972, The analytic signal of two-dimensional magnetic bodies with polygonal cross-section: Its properties and use for automated anomaly interpretation: Geophysics, **37**, 507–517, doi: 10.1190/1.1440276.

Nagy, D., G. Papp, and J. Benedek, 2000, The gravitational potential and its derivatives for the prism: Journal of Geodesy, **74**, 552–560, doi: 10.1007/s001900000116.

Pasteka, R., R. Karcol, D. Kusnirak, and A. Mojzes, 2012, REGCONT: A matlab based program for stable downward continuation of geophysical potential fields using Tikhonov regularization: Computers and Geosciences, **49**, 278–289, doi: 10.1016/j.cageo.2012.06.010.

Reginska, T., 1996, A regularization parameter in discrete ill-posed problems: SIAM Journal on Scientific Computing, **17**, 740–749, doi: 10.1137/S1064827593252672.

Salem, A., S. Masterton, S. Campbell, J. D. Fairhead, J. L. Dickinson, and C. A. Murphy, 2013, Interpretation of tensor gravity data using an adaptive tilt angle method: Geophysical Prospecting, **61**, 1065–1076, doi: 10.1111/1365-2478.12039.

Salem, A., and D. Ravat, 2003, A combined analytic signal and Euler method (AN-EUL) for automatic interpretation of magnetic data: Geophysics, **68**, 1952–1961, doi: 10.1190/1.1635049.

Salem, A., D. Ravat, M. F. Mushayandebvu, and K. Ushijima, 2004, Linearized least-squares method for interpretation of potential-field data from sources of simple geometry: Geophysics, **69**, 783–788, doi: 10.1190/1.1759464.

Salem, A., S. Williams, D. Fairhead, R. Smith, and D. Ravat, 2008, Interpretation of magnetic data using tilt-angle derivatives: Geophysics, **73**, no. 1, L1–L10, doi: 10.1190/1.2799992.

Salem, A., S. Williams, J. D. Fairhead, D. Ravat, and R. Smith, 2007, Tilt-depth method: A simple depth estimation method using first order magnetic derivatives: The Leading Edge, **26**, 1502–1505, doi: 10.1190/1.2821934.

Thompson, D. T., 1982, EULDPH: A new technique for making computer-assisted depth estimates from magnetic data: Geophysics, **47**, 31–37, doi: 10.1190/1.1441278.

Tikhonov, A. N., and B. J. Arsenin, 1977, Solutions of ILL-posed problems: John Wiley & Sons.

Tikhonov, A. N., V. B Glasko, O. K. Litvinenko, and V. R. Melikhov, 1968, Analytic continuation of a potential in the direction of disturbing masses by the regularization method: Izvestiya Physics of the Solid Earth, **12**, 30–48 [in Russian; English translation: 738-747].

Troutman, J. L., 1983, Variational calculus with elementary convexity: Springer.

Wang, F. Q., Y. P. Song, L. F. Dong, C. F. Tao, and X. B. Lin, 2019, Magnetic anomalies of submarine pipeline based on theoretical calculation and actual measurement: IEEE Transactions on Magnetics, **55**, 1–10, doi: 10.1109/TMAG.2019.2898951.

Xu, S. Z., J. Y. Yang, C. F. Yang, P. F. Xiao, S. C. Chen, and Z. H. Guo, 2007, The iteration method for downward continuation of a potential field from a horizontal plane: Geophysical Prospecting, **55**, 883–889, doi: 10.1111/j.1365-2478.2007.00634.x.

Zeng, X. N., X. H. Li, J. Su, D. Z. Liu, and H. X. Zou, 2013, An adaptive iterative method for downward continuation of potential-field data from a horizontal plane: Geophysics, **78**, no. 4, J43–J52, doi: 10.1190/geo2012-0404.1.